Probe particles alter dynamic heterogeneities in simple supercooled systems

Ronen Zangi, Stephan A. Mackowiak, and Laura J. Kaufman[a)]
Department of Chemistry, Columbia University, New York, New York 10027

(Received 16 October 2006; accepted 28 December 2006; published online 9 March 2007)

The authors present results from molecular dynamics simulations on the effect of smooth and rough probes on the dynamics of a supercooled Lennard-Jones (LJ) mixture. The probe diameter was systematically varied from one to seven times the diameter of the large particles of the LJ mixture. Mean square displacements show that in the presence of a large smooth probe the supercooled liquid speeds up, while in the presence of a large rough probe, the supercooled liquid slows down. Non-Gaussian parameters indicate that with both smooth and rough probes, the heterogeneity of the supercooled system increases. From the analysis of local Debye-Waller factors, it is evident that the change in the dynamics of the LJ system is heterogeneous, with the largest perturbations close to the probes. Large smooth and rough probes appear to set up heterogeneities in these supercooled systems that would otherwise not occur, and these heterogeneities persist for long times. © *2007 American Institute of Physics*. [DOI: 10.1063/1.2434969]

INTRODUCTION

The dynamics of glass forming systems has long been an area of intense interest. An accumulation of experimental data and simulation results shows that supercooled, or glassy, systems comprised of molecules, colloidal particles, polymers, and hard spheres all exhibit dynamic heterogeneity. Such heterogeneity is characterized by spatial regions, or domains, that relax faster (in some cases, by orders of magnitude) than other regions in the system. However, several issues related to the nature of dynamic heterogeneity in such systems remain unresolved. These include the size of domains with a particular relaxation profile, the proximity of domains that relax on dramatically different time scales, and how, if at all, particular spatial motifs encode dynamic heterogeneity? Experimentally, a large number of studies have aimed to elucidate the time and length scales on which heterogeneities exist in supercooled systems.[1,2] In particular, recent experiments have attempted to avoid the ensemble averaging inherent in traditional techniques that may obscure a wealth of detail present on the few particle level. Indeed, in the last decade a variety of novel techniques that minimize ensemble averaging have been employed to study supercooled systems. These techniques include multidimensional nuclear magnetic resonance (NMR),[3–8] novel spectroscopic approaches,[9–13] and single molecule (SM) microscopy on small molecule and polymeric glasses[14–20] as well as confocal microscopy on colloidal glasses[21–27] and molecular dynamics simulations on simple glass forming systems.[28–33]

Most experiments that access particular subensembles in supercooled systems rely on the interrogation of a probe that is expected to mirror, or at least report on, the dynamics of the supercooled surroundings. Indeed, careful experimental studies that examine whether host dynamics can be derived from bulk probe-bearing experiments [particularly in *o*-terphenyl (OTP)] have been performed.[9,34–40] These experiments conclude that only probes with similar hydrodynamic radius and mass (and perhaps intermolecular interactions) to the system components can be expected to mirror dynamics and, in particular, dynamic heterogeneities in the surrounding system. Indeed, it is reasonable that a small enough probe will escape caging related to heterogeneous dynamics. Monitoring the rotational correlation function or translational behavior of such probes might give a result consistent with a homogeneous system. Similarly, a probe large compared to the size of the dynamic heterogeneities might average over them (in space and/or in time) and thus also have a rotational correlation function or translational mobility consistent with that of a probe in a homogeneous system.

While bulk experiments have examined how and when probes mirror dynamics of supercooled host systems, no similar systematic study has examined the question of whether probes reflect the heterogeneity of the host in SM experiments. And no studies have clearly addressed whether such probes can alter the heterogeneities of supercooled systems. Experimentally, the single molecule approach is particularly attractive for studying supercooled systems, as the single fluorophores that act as probes in these systems interrogate individual molecular scale environments. Such experiments have revealed that over long times the fluorescent probes experience a mosaic of local environments.[14,19] Though thus far only heterogeneities in rotational dynamics of supercooled systems have been successfully measured with SM techniques, theoretically both translational and rotational dynamics of the probe molecules can be studied directly with these techniques. Small molecule glass formers have thus far been the subject of only one SM experiment.[14] This experiment measured both the average rotational correlation time $\langle \tau_c \rangle$ of rhodamine 6G (R6G) in OTP and the average time a probe exists in an environment that gives rise

[a)]Author to whom correspondence should be addressed. Electronic mail: kaufman@chem.columbia.edu

to similar rotational correlation times, the exchange time $\langle\tau_{ex}\rangle$. This experiment found that R6G in OTP exhibited $\langle\tau_{ex}\rangle \approx 15\langle\tau_c\rangle$ at temperatures from T_g+2 K to T_g+10 K.[14] This result differs from that measured with (probeless) multidimensional NMR experiments, which found $\langle\tau_{ex}\rangle \approx \langle\tau_c\rangle_{OTP}$ at T_g+10 K,[41] with $\langle\tau_c\rangle_{OTP}$ referring to the correlation time of OTP itself, which is at least an order of magnitude smaller than $\langle\tau_c\rangle$ measured for R6G in OTP.[14] The SM results also lack the strong temperature dependence seen in (probe-bearing) photobleaching experiments, in which $\langle\tau_{ex}\rangle/\langle\tau_c\rangle$ decreases from more than 100 at T_g+1 K to 6 at T_g+4 K.[37,42] Such vastly differing results have provoked questions on whether the probe dynamics detailed by SM experiments directly reflect those of the host.

At this point it remains unclear how single molecule probes influence measurements in supercooled systems. In particular, it is not known whether there are any single molecule fluorophore probes that can report on the presence of dynamic heterogeneities in a supercooled system and sample the system in an unbiased manner. This is due to our lack of knowledge on whether, or the extent to which, such probes alter the dynamic heterogeneities in these systems. Systematic SM experiments exploring a range of host/probe systems could shed light on how the size ratio, mass ratio, and intermolecular interactions between the probe and surrounding molecules affect measured probe dynamics and therefore under what conditions SM probes can be expected to report on dynamic heterogeneities in an unbiased manner. However, the finite number of probe/host pairs, the inability to change one probe variable independent of the rest, and the inability to monitor the host activity in the presence of different probes limit experimental ability to answer these questions. Molecular dynamics (MD) simulations can overcome the difficulties listed above and allow systematic study of how probes report on and potentially alter dynamic heterogeneities in simple supercooled systems. While simulations of three-dimensional (3D) supercooled systems of spheres do not display the full complexity of molecular glass behavior and do not closely approach the glass transition temperature T_g,[28,29] they do allow both significant control over the host and probe properties and independent measurement of the dynamics of each. While MD simulations have been done in a variety of probe-bearing supercooled systems,[30,43–49] none have explored whether probe dynamics mirror host dynamics in a manner relevant to SM experiments and in a manner that explores how the presence of the probe potentially alters heterogeneities in the system.

In this work, we report on how probe size and roughness affect the dynamic heterogeneity of the host. We find that large probes set up long lived nonrepresentative environments around the probe. Such environments may be one explanation for why SM experiments to date have measured exchange times that are longer than those measured by probeless experiments.

SIMULATION DETAILS

The 3D system modeled consists of a probe surrounded by a supercooled liquid. The model for the supercooled liquid is a binary mixture with a 4:1 ratio of A and B particles: the Lennard Jones (LJ) mixture.[28–30] The particles interact via a LJ potential, $V_{\alpha\beta}(r)=4\varepsilon_{\alpha\beta}[(\sigma_{\alpha\beta}/r)^{12}-(\sigma_{\alpha\beta}/r)^6]$, with $\varepsilon_{AA}=1$ and $\sigma_{AA}=1$ for interactions between the A particles and $\varepsilon_{BB}=0.5\varepsilon_{AA}$ and $\sigma_{BB}=0.88\sigma_{AA}$ for interactions between the B particles. The LJ parameters between the A and B particles, $\varepsilon_{AB}=1.5\varepsilon_{AA}$ and $\sigma_{AB}=0.80\sigma_{AA}$, ensure that the system will not crystallize. The masses of the mixture particles were taken to be $m_A=m_B=1.0$. The simulations were carried out, and the results are reported below, in terms of the reduced variables $r^*=r/\sigma_{AA}$, $m^*=m/m_A$, $T^*=k_BT/\varepsilon_{AA}$, and $t^*=t(k_BT/m_A\sigma_{AA}^2)^{1/2}$.

TABLE I. Length (L^*) of a side of the simulation box and pressure (P^*) of the simulated system containing smooth probes with $\sigma_P=1.0-7.0$ at two temperatures $T^*=0.48$ and $T^*=0.70$.

	$T^*=0.48$		$T^*=0.70$	
σ_P	L^*	P^*	L^*	P^*
1.0	13.617	1.76	13.777	2.97
2.0	13.624	1.85	13.787	2.91
3.0	13.650	1.82	13.810	2.95
4.0	13.691	1.78	13.852	2.88
5.0	13.760	1.83	13.919	2.82
6.0	13.854	1.79	14.018	2.76
7.0	13.995	1.84	14.154	2.75

Two types of probe are considered in this study. The first is a smooth probe represented by a single particle with LJ parameters $\varepsilon_P=1.0$ and different values of σ_P. A set of seven simulations with $\sigma_P=1.0$, 2.0, 3.0, 4.0, 5.0, 6.0, and 7.0 was performed to model probes with different sizes but with the same mass, $m_P=4.0$. In addition, probes with $\sigma_P=3.0$, 5.0, and 7.0 with $m_P=27$, 125, and 343, respectively, were employed to investigate the effect of probe mass. Since the value of σ_P was considered to be as high as 7.0, the interparticle potentials and the corresponding forces in the range of $4.0\leqslant r^*\leqslant 5.0$ were interpolated from their LJ values at $r^*=4.0$ to zero at $r^*=5.0$ by a third degree polynomial. The same number of mixture particles are taken, $N_A=2400$, $N_B=600$, and $N_P=1$, for the simulations with different σ_P; however, the volume of the cubic simulation box was adjusted so that the measured pressure was similar (Table I). A set of simulations was also attempted in which the volume of the box was varied to attain constant volume fraction ϕ with $\phi=(N_Ar_A^3+N_Br_B^3+N_Pr_P^3)/V$ with the radii of the particles determined from the corresponding LJ parameter σ for the different σ_P. However, the properties (e.g., the mean square displacement) of particles far from the probe (in regions that can be considered "bulk") were not the same for systems with probes of different sizes. In addition, the pressure of these systems was found to be significantly different. This is the reason why we performed the simulations such that pressure, rather than volume fraction, was kept constant between simulations with different σ_P. The resulting reduced densities, $\rho^*=N/V^*$, of such systems can be calculated from values in Table I and are $\rho^*=1.188$ for the system with $\sigma_P=1$ and $T^*=0.48$ and $\rho^*=1.148$ for the system with $\sigma_P=1$ and $T^*=0.70$. The LJ parameters of the probe with the mixture

particles were calculated from the geometric combination rule of the parameters associated with the mixture particles ($\sigma_{AA}, \sigma_{BB}, \varepsilon_{AA}, \varepsilon_{BB}$) and the LJ parameters of the probe.

The second type of probe investigated is a rough probe. The probe was modeled as a cluster of N_{PC} particles strongly attracted to each other. Each particle within the probe will be termed a probe-component particle and notated with subscript "PC" and the agglomeration of such particles is termed the probe and denoted with subscript "P." In this case, the total number of particles in the system ($N=2985$) was constant for a set of simulations with probes composed of a different number of particles $N_{\mathrm{PC}}=25$, 50, 100, and 200. This was done by equilibrating a system of the supercooled liquid with $N_A=2388$ and $N_B=597$ in a cubic box with a length $L^*=13.55$, yielding a reduced density of $\rho^*=1.2$. Then, N_{PC} probe-component particles were introduced by reidentifying $(4N_{\mathrm{PC}}/5)A$ and $(N_{\mathrm{PC}}/5)B$ particles of the mixture as probe-component particles. The A and B particles that were replaced with the probe-component particles were in most cases nearest neighbors of each other. The mass of each probe component was $m_{\mathrm{PC}}=1.0$. The LJ parameters used for the interactions between the probe components were $\sigma_{\mathrm{PCPC}}=0.96$ (a weighted average of the diameters of the mixture particles) and $\varepsilon_{\mathrm{PCPC}}=4.0$ (a deep potential well to keep the probe components "bound" to each other). The LJ parameters of the probe-component particle interactions with the binary supercooled liquid were set to $\sigma_{\mathrm{PC}A}=0.98$ and $\varepsilon_{\mathrm{PC}A}=1.0$ and $\sigma_{\mathrm{PC}B}=0.92$ and $\varepsilon_{\mathrm{PC}B}=0.707$. The strength of the interactions between the probe components and the binary mixture is similar to the strength of the interactions between the particles of the glassy mixture. In this set of simulations, the interparticle potentials and the corresponding forces in the range of $3.0 \leqslant r^* \leqslant 4.0$ were interpolated from their LJ values at $r^*=3.0$ to zero at $r^*=4.0$ by a third degree polynomial. For $r^*>4.0$, the interparticle potential was set to zero. This potential is set to zero at a smaller distance than in the case of the smooth probe ($r^*>5.0$) because this potential is calculated from each probe-component rather than the center of mass of the probe as it is for the smooth probe.

The MD simulations are performed using the GROMACS package Version 3.2.1.[50] For each simulation the system is equilibrated for at least 10^7 MD steps. The simulations are performed in the microcanonical ensemble (N,V,E), except for the preparation stage where the Berendsen thermostat is applied to obtain the desired temperatures[51] of $T^*=0.48$ and 0.70. The data collection step consisted of short and long simulations. The short simulations were run for 1.6×10^5 MD steps with time step $\delta t^*=0.0025$, where the trajectory was saved every 8 MD steps. The long simulations were run for 10^7 MD steps with $\delta t^*=0.01$, and the trajectory was saved every 500 MD steps.

To characterize the translational mobility of the system, the mean square displacements (MSDs) and non-Gaussian parameters for the A mixture particles were calculated. The MSD is given by $\langle(\mathbf{r}(0)-\mathbf{r}(t))^2\rangle$, and the 3D non-Gaussian parameter is defined as $\alpha_2(t)=\frac{3}{5}\langle\delta\mathbf{r}^4\rangle/\langle\delta\mathbf{r}^2\rangle^2-1$, with $\delta\mathbf{r}$ the distance a particle moves in time t. To characterize the dis-

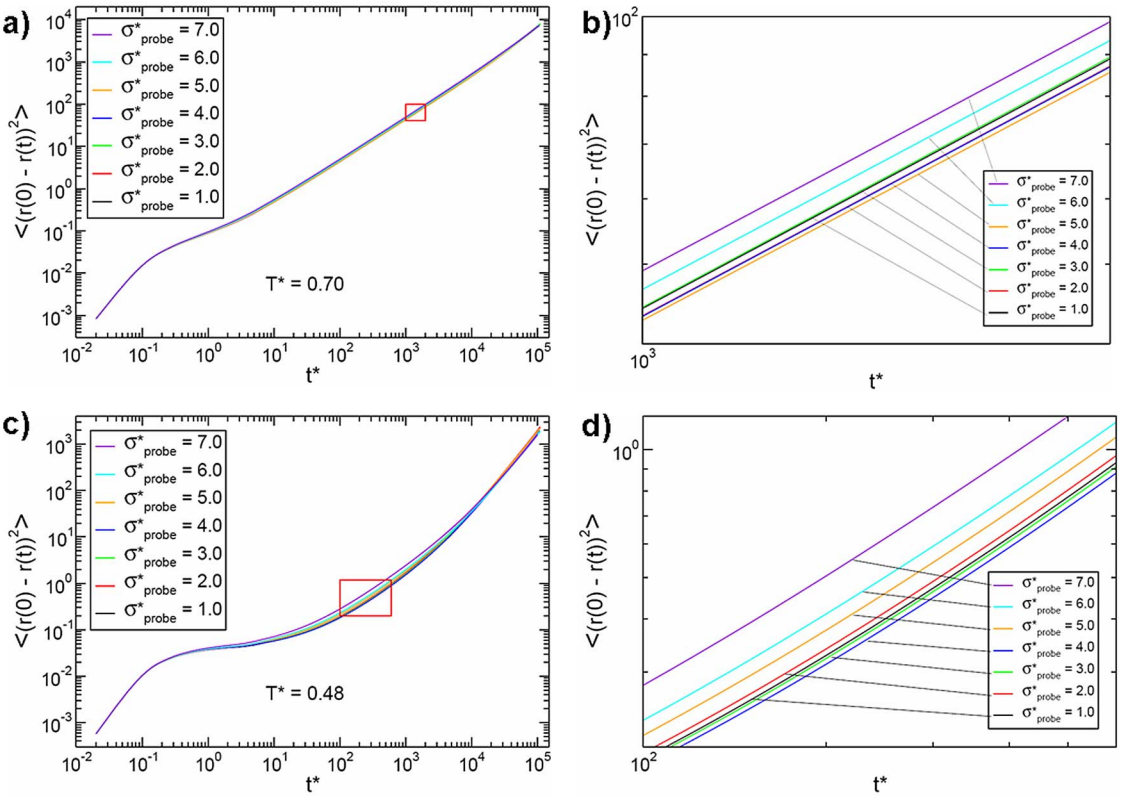

FIG. 1. (Color online) (a) Mean square displacement (MSD) for A particles of a binary Lennard-Jones (LJ) system surrounding smooth spherical probes from $\sigma_{\mathrm{P}}=1$ (size of the larger component of the LJ system) to $\sigma_{\mathrm{P}}=7$ at $T^*=0.70$. (b) Expanded view of area enclosed by box in (a). (c) MSD for A particles in the presence of smooth spherical probes at $T^*=0.48$. (d) Expanded view of area enclosed by box in (c) In both cases, in the late β regime the systems containing large probes display increased motion and reduced caging behavior in the presence of large probes.

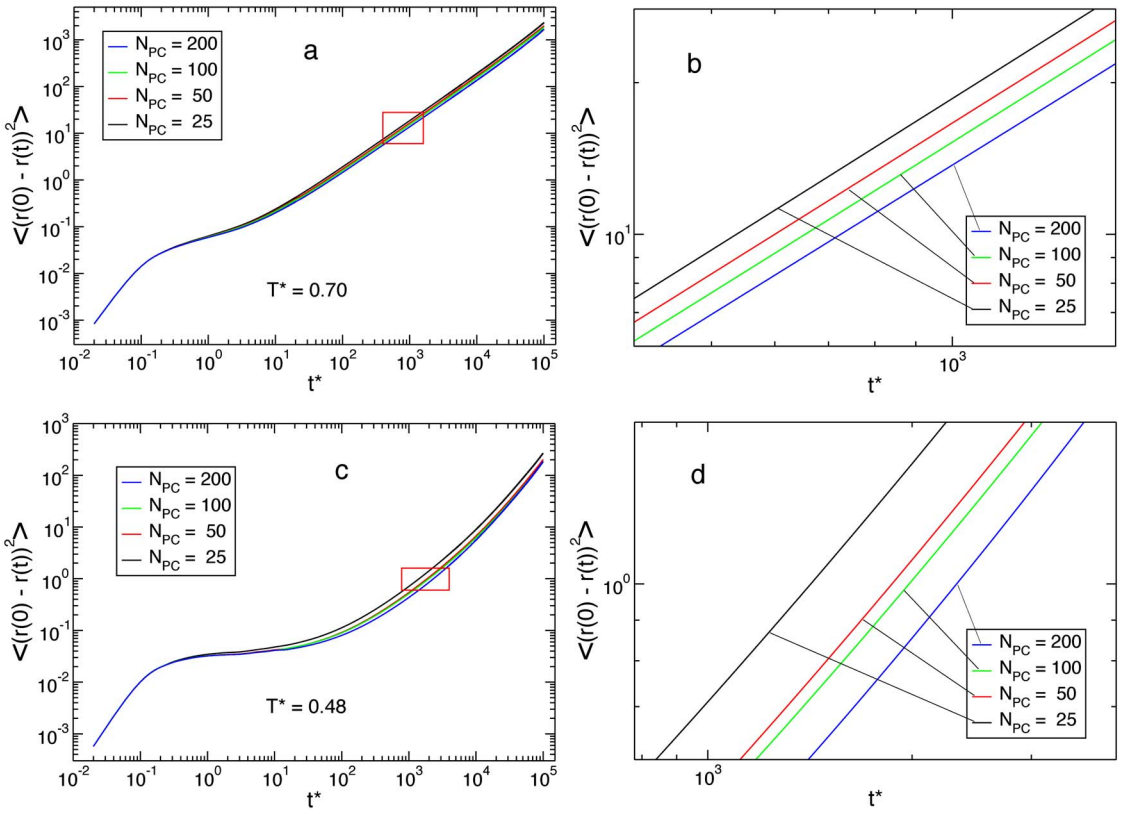

FIG. 2. (Color online) (a) MSD for A particles of a binary LJ system surrounding rough spherical probes composed of clusters with 25–200 LJ spheres at $T^*=0.70$. (b) Expanded view of area enclosed by box in (a). (c) MSD for A particles in the presence of rough probes at $T^*=0.48$. (d) Expanded view of area enclosed by box in (c). A probe with $N_{PC}=25$ corresponds to $\sigma^*\sim 3.8$ and a probe of $N_{PC}=200$ corresponds to $\sigma^*\sim 7.2$. In both cases, in the late β regime and early α regime the systems containing large probes exhibit decreased motion and increased caging behavior in the presence of large probes.

placement of the mixture particles at short times, Debye-Waller factors for each particle i are calculated by

$$\mathrm{DW}_i = \langle\langle(\mathbf{r}_i(t) - \langle\mathbf{r}_i\rangle_\tau)^2\rangle_\tau\rangle,$$

where $\langle\cdots\rangle_\tau$ denotes an average over time period τ^*, and the outer brackets, $\langle\cdots\rangle$, denote an average over the (short) simulation trajectory. The distance of each particle from the center of mass of the probe calculated at the beginning of each time interval τ^* was used to plot the Debye-Waller factor as a function of distance from the probe, $\mathrm{DW}(\mathbf{r})=\langle \mathrm{DW}_i\cdot\delta(\mathbf{r}-(\mathbf{r}_i-\mathbf{r}_\mathrm{P}))\rangle$.

RESULTS AND DISCUSSION

Mean square displacements and non-Gaussian parameters for the A particles in the binary mixture in the presence of a single mobile smooth probe have been calculated at a number of different temperatures. Probe size was varied between $\sigma_\mathrm{P}=1.0$ and $\sigma_\mathrm{P}=7.0$. A system with $\sigma_\mathrm{P}=1.0$ is similar to a probeless system in that the tagged particle has the same diameter as the A particles in the mixture, but the probe has a larger mass ($m_\mathrm{P}=4$ vs $m_A=1$). Figure 1 shows the MSD results for the A particles of systems containing smooth probes at two temperatures, $T^*=0.70$ and $T^*=0.48$. At $T^*=0.70$, the MSD shows some evidence of the onset of caging behavior, as can be seen in the small shoulder in the MSD most apparent between $0.1<t^*<1$. This is consistent with the findings of Kob and Andersen.[28] At longer times, there is recovery of diffusive motion. As can be seen from Fig. 1(a), the MSD of the A particles of the system increases more quickly with time in the presence of probes with $\sigma_\mathrm{P}\geqslant 6.0$ than in the presence of smaller probes. Figure 1(b) shows that the diffusion constant for the A particles in the presence of the two largest probes is indeed larger than that in the presence of the smaller probes (with the diffusion constant being proportional to the y intercept on the log-log plot of the MSD versus time).

The acceleration of the supercooled system in the presence of large smooth probes becomes clearer at lower temperatures, as can be seen in Fig. 1(c). At $T^*=0.48$, the MSD exhibits a clear plateau, which persists an order of magnitude longer than at $T^*=0.70$. For the purposes of this manuscript, we identify the range of time between that at which the plateau begins and that at which the MSD reaches ~ 1 as belonging to the β regime, in which caging dominates the dynamics. The time regime beyond that is identified as the α regime, the time scale over which the average particle escapes its cages, and the MSD becomes linear in time. The plateau in the MSD at $T^*=0.48$ occurs at $t^*\sim 0.25$, corresponding to a distance of $r^*\sim 0.17$, much smaller than any of the particles in the system and consistent with caged behavior. At $T^*=0.48$, subdiffusive behavior persists until $t^*\sim 10^3$. In the late β and early α regimes there is a clear increase in the MSD value and an earlier escape from the cage (or divergence from the plateau) as the size of the smooth probe increases. Appreciable differences are seen in systems with

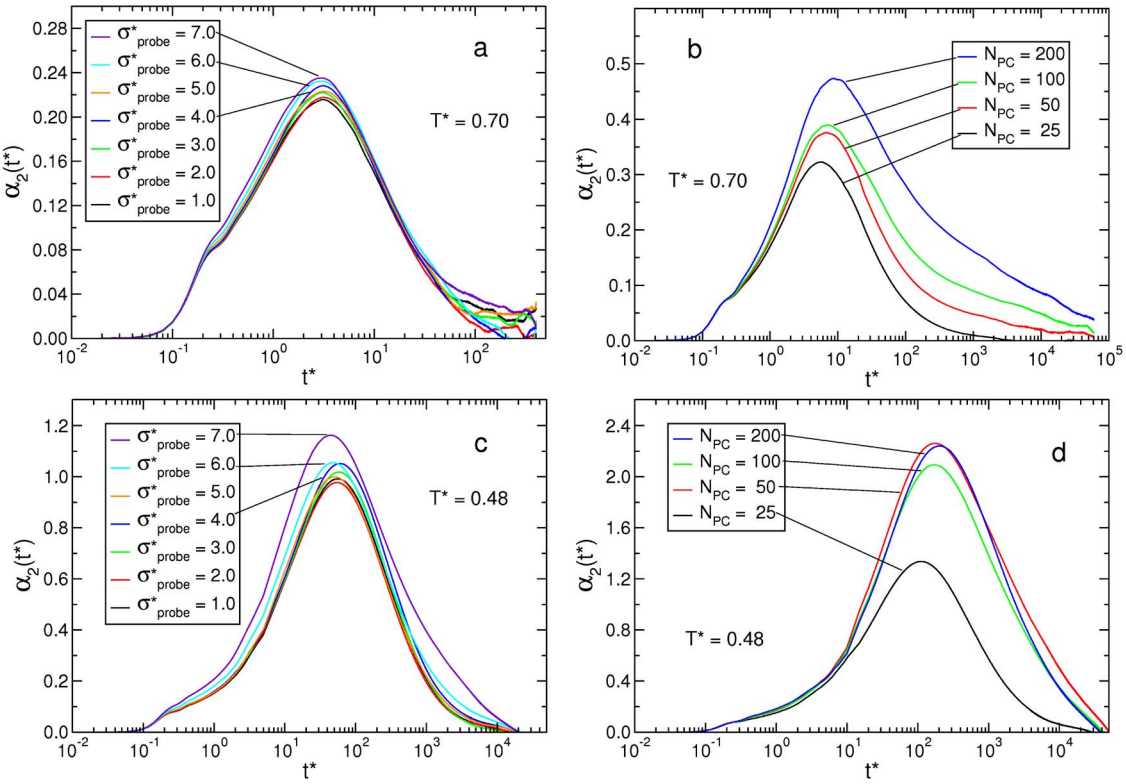

FIG. 3. (Color online) Non-Gaussian parameters of the *A* particles of a binary LJ system with (a) smooth and (b) rough probes at (a) $T^*=0.70$. Non-Gaussian parameters of *A* particles of a binary LJ systems with (c) smooth and (d) rough probes at $T^*=0.48$.

probes of $\sigma_P \geqslant 4$, though it should be noted that at the longest times measured, the MSDs converge. The probe size at which differences are evident depends on system size, and in the limit of infinite dilution (one large probe particle in an infinitely large supercooled mixture) any perturbation due to the probe particle would not be apparent in examining bulk quantities of the entire mixture. However, it remains clear that in finite systems, the presence of a large smooth, mobile probe in a 3D supercooled system accelerates motion in the system.

Moving to rough probes, which are prepared as described in the Simulation Details section, the findings are inverted. Figure 2 shows the MSDs for the *A* particles comprising the supercooled system for rough probes with $N_{PC}=25$, 50, 100, and 200. Because these rough probes are comprised of probe-component particles held together by LJ potentials with $\varepsilon_{PCPC}=4$, they do not dissociate. However, there is some movement among the particles, particularly at higher temperatures, and irregularities on the surface preclude absolute assignment of a diameter to these probes. However, the probes with 25, 50, 100, and 200 component particles have approximate diameters as determined by the first peak of the corresponding probe-mixture radial distribution functions at $T^*=0.7$ of $\sigma_P \sim 3.8$, 4.6, 6.0, and 7.2, respectively. Unlike the smooth probes, these rough probes have masses that increase with probe size and thus range from $m_P=25$ to 200. Figure 2 shows that at both $T^*=0.70$ and $T^*=0.48$, the particles within the supercooled systems spend more time in the β regime and recover diffusive behavior later as the size of the probe increases. Thus, the presence of a large rough, mobile probe slows the overall translational mobility of the supercooled system. Here, the changes in MSD as a function of probe size are stronger than in the systems with smooth probes. In addition, there is persistence of the decreased translational mobility of supercooled systems containing the largest probes even at the longest times measured.

Figure 3 shows the non-Gaussian parameters, $\alpha_2(t)=\frac{3}{5}\langle \delta \mathbf{r}^4\rangle/\langle \delta \mathbf{r}^2\rangle^2-1$, with $\delta \mathbf{r}$ the distance a particle moves in time t, for the same systems for which the MSDs were plotted in Figs. 1 and 2. Again, the plots show the results for the *A* particles of the mixture. The non-Gaussian parameter generally peaks at a time similar to that at which the MSD upturn in the late β regime occurs. The peak in the non-Gaussian parameter then also corresponds to the time at which an average particle escapes its cage and has been shown to correspond approximately to the time at which the dynamic heterogeneity in the sample is a maximum. The width of the non-Gaussian parameter reflects the breadth of time scales over which dynamic heterogeneity is present. The height of the non-Gaussian parameter reports on the magnitude of heterogeneous behavior in the system, with a larger peak height chiefly reflecting the behavior of "mobile" particles that move farther than expected from a Gaussian distribution of particle displacements.[52] Figure 3 shows that at both high and low temperatures, in the presence of smooth probes, the non-Gaussian parameter peaks earlier with increasing probe size. This is consistent with the fact that diffusive behavior is recovered more quickly in these systems than in systems with small probes, as seen in the MSDs. In the presence of rough probes, the finding is inverted, and generally as the probe size increases, at both $T^*=0.70$ and

$T^*=0.48$, the non-Gaussian parameters peak later and have larger widths. Again, this is consistent with the later upturn in the MSDs as the size of the rough probe increases. However, while the peak positions display opposite behavior in the presence of large smooth and large rough probes, for both types of probes, the height of the non-Gaussian parameter increases as a function of probe size. As seen in the MSDs, changes in dynamics as a function of probe size are more obvious in the presence of rough than smooth probes. Indeed, the non-Gaussian parameters for systems with rough probes increase much more obviously as a function of probe size than do those for systems with smooth probes. Even though, in general, the changes of non-Gaussian parameter with probe size are clearer in rough probes than in smooth probes, Fig. 3(d) shows that for rough probes at $T^*=0.48$, the peak of $\alpha_2(t)$ is highest for the $N_P=50$ probe, not the $N_P=200$ probe. This may be due to finite system size and finite simulation time effects as will be described below. The increase in peak height of α_2 in systems with both smooth and rough probes shows that the presence of a large probe increases heterogeneity in the system, no matter if on average the probe is causing the particles comprising the supercooled system to speed up or slow down.

The increased heterogeneity in these systems, as well as the behavior illustrated in Figs. 1 and 2, can be understood by examining two-dimensional (2D) projections of the 3D trajectories of particles surrounding rough and smooth probes of a variety of sizes. Figure 4 shows such trajectories around a smooth probe with $\sigma_P=2$ ($L^*=13.48$), a smooth probe with $\sigma_P=5$ ($L^*=13.69$), and a rough probe with $N_{PC}=100$ and $\sigma_P\sim 6$ ($L^*=13.46$), all at $T^*=0.44$. It should be noted that the systems shown here differ slightly from the systems for which the MSD and non-Gaussian parameters are calculated. Here, instead of ensuring that the pressures are the same, the volume fractions of the systems are fixed and the volume of the box changes accordingly with probe size. The reduced density of this system is 1.23, slightly higher than the density of 1.2 in a probeless LJ system and than that in the systems that give rise to Figs. 1–3. This higher density results in slightly larger differences in MSD and larger heterogeneities as reflected in α_2 as a function of probe size than in the systems described by Table I. It also allows the differences in trajectories between particles near and far from the probe to be seen more clearly in 2D projections of the 3D trajectories. These systems display the same trends in MSD and α_2, as those illustrated in Figs. 1–3. The trajectories plotted in Fig. 4 are for a mobile probe. However, they are displayed relative to the probe position, so the probe appears to remain fixed in the center of the box at all times. For Fig. 4(a), with $\sigma_P=2.0$, the time interval depicted is $t^*=2\times10^4$, and the frames are separated by $dt^*=10^3$. In Fig. 4(b), with $\sigma_P=5.0$, the time interval is $t^*=800$, and the frames are separated from each other by $dt^*=40$. For Fig. 4(c), with $N_{PC}=100$, $t^*=1.6\times10^4$, with $dt^*=800$. These intervals all correspond to times near the upturn in the MSD of these systems, which differ from those shown in Figs. 1 and 2 for the reasons discussed above.

Comparison of Figs. 4(a) and 4(b) shows that in systems with large smooth probes, the motion of the particles closest

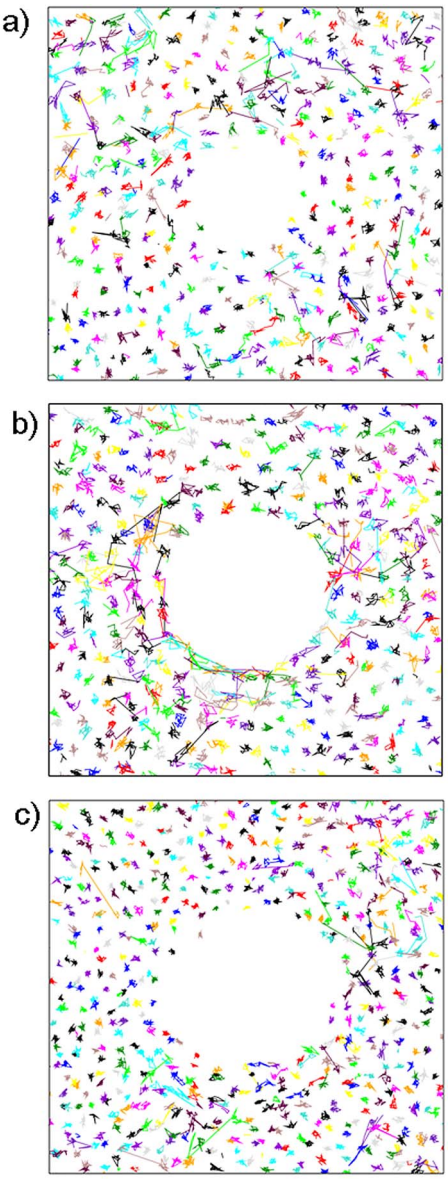

FIG. 4. (Color online) 2D projections of 3D trajectories of LJ particles surrounding (a) a smooth probe with $\sigma_P=2.0$, $t^*=2\times10^4$, and frames separated by $dt^*=10^3$; (b) a smooth probe with $\sigma_P=5.0$, $t^*=800$, and $dt^*=40$; and (c) a rough probe with $N_{PC}=100$ and $\sigma^*\sim6.0$, $t^*=1.6\times10^4$, and $dt^*=800$. All systems are at $T^*=0.44$. These systems are similar to those for which the MSDs in Figs. 1 and 2 are calculated (see text for details).

to the probe is different in character than those farthest from the probe and also different in character than any of those in a system containing a small probe or, presumably, no probe at all. Indeed, the particles closest to the probe in Fig. 4(b) appear to be more mobile on average than both particles far from the large probe or particles near or far from a small smooth probe. Furthermore, the trajectories of particles in the nearest shells around the large smooth probe tend to be anisotropic and stringy, with relatively little motion orthogonal to the tangent of the projection of the probe and significant motion along the shell defined by the probe. This increased motion around the probe is the source of the increase in the MSD at intermediate times displayed in Fig. 1. The fact that Fig. 1 shows that supercooled systems in the presence of smooth probes have MSDs that converge at the long-

est times studied is consistent with this explanation for the increase in the MSDs at intermediate times: by the longest times investigated, even those particles displaying increased propensity for motion in shells around the probe at intermediate times have randomized spatially and thus recover bulk behavior associated with probeless systems of the same density and temperature. Figure 4(c) shows behavior dissimilar to that illustrated in Fig. 4(b). Here, the particles nearest the large rough probe tend to have very compact trajectories compared to those far from the probe. We believe that this lack of mobility of particles near a rough probe leads to the extended β regime compared to that in smooth probe-bearing systems, as seen in Figs. 1 and 2.

The behavior illustrated in Fig. 4 also explains both the shift in peak position and magnitude in the non-Gaussian parameters as a function of probe size and roughness. For smooth (rough) probes, the peak of α_2 moves to shorter (longer) times with increasing probe size for the same reason the upturn out of the plateau in the MSD occurs earlier (later) in those systems. However, the increase of peak height of α_2 indicates an increase in heterogeneity in systems with both smooth and rough probes. This is presumably because the presence of the probe allows for the existence of a subset of particles surrounding it that are faster (slower) than would be any set of particles in the system on average in the absence of a smooth (rough) probe while allowing the full range of supercooled heterogeneous dynamics in regions far from the probe. For the rough probe of $N_{PC}=50$ at $T^*=0.48$, we find that the height of α_2 does not fit the trend. Though we do not fully understand the origin of this behavior, it may be due to the fact that large rough probes so strongly affect the dynamics of their surroundings that even on the longest time scales interrogated a substantial fraction of particles in the system do not experience the full range of dynamics available to particles in a probeless system at the same density and temperature. Such an explanation is consistent with the fact that the rough probe MSDs at $T^*=0.48$ do not converge at the longest times measured [Fig. 2(c)], unlike those for systems with smooth probes [Fig. 1(c)].

To quantify the changes in the translational mobility of LJ particles surrounding both smooth and rough probes, Debye-Waller (DW) factors were calculated for every particle as described in the Simulation Details section at both $T^*=0.70$ and $T^*=0.48$. Binning was then performed to investigate the particle DW factors as a function of distance $\mathbf{r}$ from the center of mass of the probe. For the smooth probes, bins are $0.20\sigma_{AA}$ wide and start at the perimeter of the probe. For rough probes, bins are $0.39\sigma_{AA}$ wide and start at the perimeter of the probe, which due to the nature of the probe is slightly temperature dependent. It has been shown recently that DW factors at intermediate time scales (β regime) are reflective of long time dynamic propensities, with the propensity being a measure of the probability of a particle in a particular spatial configuration undergoing a substantial displacement in a given time.[53,54] Though we do not explore isoconfigurations as do Widmer-Cooper and Harrowell, we average particle DW factors for shells of particles as a function of distance from the probe, which provides a way to predict probabilities of displacement of particles as a function of distance from the probe without running long trajectories. Figures 5 and 6 show DW($\mathbf{r}$) for the A and B mixture particles of the LJ systems with smooth and rough probes that give rise to Figs. 1–3. At $T^*=0.48$ and $T^*=0.70$, the times over which DW($\mathbf{r}$) is calculated are $\tau^*=2.0$ and $\tau^*=1.0$, respectively. These times fall in the β, or subdiffusive, regime. LJ particles far from smooth probes at both high and low temperatures exhibit average DW factors that are identical regardless of probe size (~ 0.022 at $T^*=0.70$ and ~ 0.016 at $T^*=0.48$). However, there are clear increases of DW($\mathbf{r}$) for mixture particles in the vicinity of probes with $\sigma_P \geq 4$. For $\sigma_P=7$, the DW factor near the probe is more than twice that of the system with $\sigma_P=1$. Furthermore, the increase in DW factor relative to that of the system with $\sigma_P=1$ persists until approximately the third shell of particles surrounding the probe. The magnitude of the increase and persistence as a function of distance from the probe is similar at both temperatures. Some oscillation is seen in DW($\mathbf{r}$) in the systems with smooth probes of all sizes. With binning every $r^*=0.20$, this oscillation is reflective of the radial distribution function of these systems: slightly higher DW factors occur in shells where the particle density is lower. In

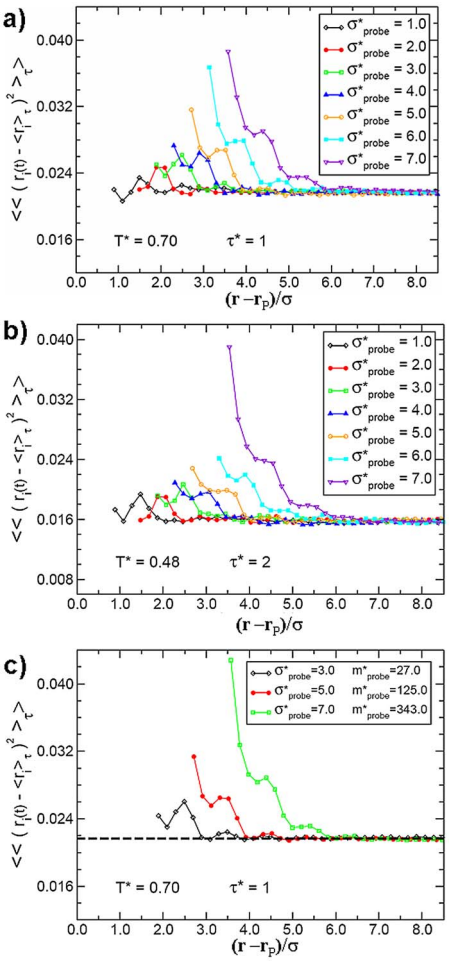

FIG. 5. (Color online) Radially binned Debye-Waller factors [DW($\mathbf{r}$)] for (a) smooth probes from $\sigma_P=1.0$ to 0.70 at $T^*=0.7$ for $\tau^*=1$ and (b) smooth probes from $\sigma_P=1.0$ to 7.0 for $T^*=0.48$ and $\tau^*=2$. (c) Radially binned DW factors for smooth probes of $\sigma_P=3.0$, 5.0, and 7.0 with $m_P=27$, 125, and 343, respectively. The dashed line indicates plateau value of DW($\mathbf{r}$) for smooth probes of $m_P=4$ shown in (a).

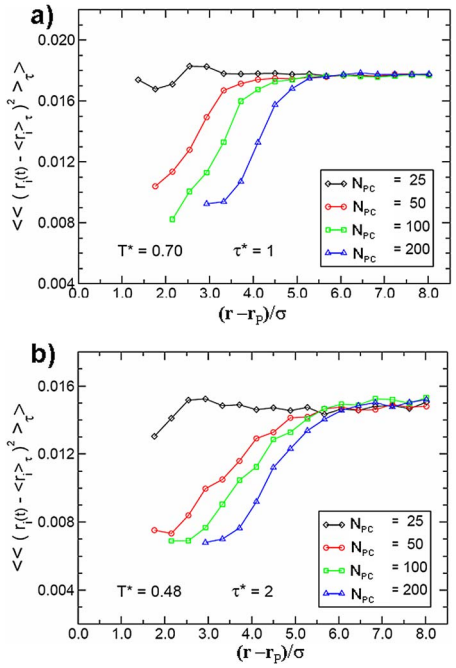

FIG. 6. (Color online) Radially binned Debye-Waller factors [DW(**r**)] for rough probes from $N_{PC}=25$ to 200 for (a) $T^*=0.70$ and $\tau^*=1$ and (b) $T^*=0.48$ and $\tau^*=2$.

rough probes, oscillations are not apparent because the probes are not uniform and the surface roughness broadens peaks in the radial distribution function significantly relative to those of systems containing smooth probes. In contrast to the behavior in systems with smooth probes, for systems with rough probes, the DW factors are smaller near the probe than far from it. The magnitude and persistence with r^* of the change in DW factors as a function of probe size is similar to that seen for the systems with smooth probes. The DW factors far from the rough probes plateau at DW(**r**)$\sim$0.015 and 0.018 at $T^*=0.48$ and $T^*=0.70$, respectively. The fact that these DW factors are smaller than those for the smooth probes is related to the slightly different sample preparation that leads to the overall density in the rough probe samples being 1.2, whereas that of the smooth probes is less than 1.2. The magnitude of the DW factors in the vicinity of large rough probes varies from $\frac{1}{2}$ to $\frac{1}{3}$ that of the plateau DW factor, indicating that the rough probes alter heterogeneities in supercooled systems more than smooth probes of the same size. This can also be seen in the substantial difference in DW(**r**) between systems with $N_{PC}=25$ and $N_{PC}=50$, which have $\sigma_P\sim3.8$ and $\sigma_P\sim4.6$, respectively.

As discussed previously, while the smooth probes of all sizes have $m_P=4$, the rough probes have masses that range between $m_P=25$ and $m_P=200$. Though mass does not show up in the Stokes-Einstein relation or in the definition of diffusion constant, it can influence the transport properties of particles in binary systems under certain circumstances.[48,49,55–57] To interrogate whether the slowing of the surroundings in the presence of large rough probes relative to large smooth probes is due to mass, the translational mobilities of the binary mixture of systems with smooth probes with $\sigma_P=3$, 5, and 7 and $m_P=27$, 125, and 343, respectively, were investigated. MSDs (not shown), non-Gaussian parameters (not shown), and DW factors [Fig. 5(c)] show that mass does not affect the behavior of LJ particles in the presence of smooth probes. Indeed, Figs. 5(b) and 5(c) show that DW(**r**) is essentially indistinguishable in the systems with heavy, smooth probes and those with $m_P=4$ smooth probes. This shows that mass is not responsible for the differences in MSD, non-Gaussian parameter, and DW factors that occur between large smooth and large rough probes, which differ not only in roughness but also in mass.

Our findings of increased probability for mobility of particles, comprising a supercooled system in the presence of large smooth probes and decreased propensity for mobility of particles in such a system in the presence of large rough probes, are consistent with previous simulations that investigated the behavior of rough solutes in a dense fluid of spherical solvent particles[58] and the behavior of supercooled systems in the vicinity of smooth and rough walls.[59–61] Here, it was found that dynamics of a supercooled system close to a rough wall are slowed by orders of magnitude, and dynamics close to a smooth wall are accelerated by a similar amount even in the absence of any change in the structural properties of the system. This indicates that it is not solely the glass structure that encodes dynamics in supercooled systems. The studies on the effect of smooth and rough walls on the properties of supercooled liquids have indicated that not only dynamics near the wall but also melting temperature is altered in the presence of a proximate wall.[62–64] However, since some of these studies were performed on systems with walls only a few particle diameters apart, the confined nature of the system precludes direct inference to the system we are studying here. Nevertheless, in the simulations presented here, the origin of the dynamical changes near large probes is likely very similar to that near a wall, though we find these changes in the presence of mobile probes as opposed to the static walls studied previously. Despite the fact that the probes investigated are mobile, their long time diffusion constants can be expected to be smaller than that of the rest of the particles in the system in accordance with the Stokes-Einstein relation that predicts $D_{trans}\propto r^{-1}$, with r the radius of the probe. Thus, particles next to a probe can be approximated by particles adjacent to a curved wall. The fact that a large smooth probe can, to a certain extent, melt a glass and that a large rough probe can induce glassiness is related to the fact that collective motions are necessary to allow for relaxations in the high density environments of supercooled liquids. Against a rough probe, as has been constructed for this study, any neighboring particle is in an environment that structurally appears very similar to that of a probeless system. Here, however, the probability that a fluctuation involving multiple particles that allow particles neighboring the probe to exhibit cage escape is diminished. This is due to the fact that the probe exhibits very little overall motion and very few vibrations between the particles that comprise the probe because of the deep energy well keeping the components of the probe together. The probe effectively pins nearby particles, and the effectively trapped first shell around the probe provides a slightly less stringent pinning of the next shell and so on for several shells surrounding the probe.

Against a smooth wall, the situation appears to be somewhat less intuitive. The particles near a large smooth probe are not in an environment similar to the one they would be in the absence of the probe. Indeed, the smooth probe provides a slip boundary condition parallel to the tangent of the probe surface but a stick boundary condition perpendicular to the tangent of the probe. Furthermore, near a smooth wall or smooth large probe, there is little caging provided by the structure of the probe itself, and a fluctuation along the tangent of the probe will provide a path for collective motion in this direction, which in turn facilitates large displacements. These factors come together to diminish the motion of the particles comprising the supercooled system perpendicular to the probe while greatly accelerating them along the probe.

CONCLUSION

The MSD and peak position of non-Gaussian parameters for a simple supercooled system containing a large smooth probe show that the overall system speeds up. It is apparent that particles in the vicinity of the large smooth probe are more mobile than are those far from the probe, which show heterogeneities typical of probeless systems in these conditions. This is confirmed by the DW factor measurements that show that a particle's probability for motion is maximized near large smooth probes. In the presence of rough probes, these finding are inverted: the larger the probe, the slower the surrounding host particles, as reflected in the MSD, peak position of non-Gaussian parameter, and DW factors. All systems with large probes exhibit increased heterogeneity relative to probeless systems at the same density and temperature, whether the probe induces an acceleration or a slow down. These results demonstrate for the first time that large probes not only do not necessarily sample heterogeneous dynamics in an unbiased manner but also can alter heterogeneous dynamics. These results also suggest one reason why SM experiments have measured long and relatively temperature-independent exchange times: the large probe sets up and preferentially reflects the dynamics of a local environment that may not otherwise exist. While these results are intriguing, further investigation to determine under what circumstances probes alter the dynamics and heterogeneities of supercooled systems is necessary. In addition to exploring how probe size, roughness, and mass affect heterogeneities in these simple supercooled systems, energetic interactions between host and probe particles must be considered. In this study we minimized this effect by setting probe-host interactions similar to host-host interactions. In addition, future work should explore probe diffusion together with host dynamics to understand how significantly alterations in heterogeneities influence probe dynamics and to what extent probe dynamics in any probe-bearing system can be expected to reflect behavior of the supercooled system.

ACKNOWLEDGMENT

The authors thank D. R. Reichman for helpful discussions.

[1] H. Sillescu, J. Non-Cryst. Solids **243**, 81 (1999).
[2] H. Sillescu, R. Bohmer, G. Diezemann, and G. Hinze, J. Non-Cryst. Solids **307–310**, 16 (2002).
[3] K. Schmidtrohr and H. W. Spiess, Phys. Rev. Lett. **66**, 3020 (1991).
[4] U. Tracht, M. Wilhelm, A. Heuer, H. Feng, K. Schmidt-Rohr, and H. W. Spiess, Phys. Rev. Lett. **81**, 2727 (1998).
[5] G. Hinze, Phys. Rev. E **57**, 2010 (1998).
[6] U. Tracht, A. Heuer, and H. W. Spiess, J. Non-Cryst. Solids **235**, 27 (1998).
[7] S. A. Reinsberg, X. H. Qiu, M. Wilhelm, H. W. Spiess, and M. D. Ediger, J. Chem. Phys. **114**, 7299 (2001).
[8] X. H. Qiu and M. D. Ediger, J. Phys. Chem. B **107**, 459 (2003).
[9] M. T. Cicerone and M. D. Ediger, J. Chem. Phys. **103**, 5684 (1995).
[10] F. R. Blackburn, C. Y. Wang, and M. D. Ediger, J. Phys. Chem. **100**, 18249 (1996).
[11] D. D. Deppe, A. Dhinojwala, and J. M. Torkelson, Macromolecules **29**, 3898 (1996).
[12] R. Richert, J. Non-Cryst. Solids **235**, 41 (1998).
[13] C. J. Ellison and J. M. Torkelson, J. Polym. Sci., Part B: Polym. Phys. **40**, 2745 (2002).
[14] L. A. Deschenes and D. A. V. Bout, J. Phys. Chem. B **106**, 11438 (2002).
[15] V. Biju, J. Ye, and M. Ishikawa, J. Phys. Chem. B **107**, 10729 (2003).
[16] R. A. L. Vallee, N. Tomczak, L. Kuipers, G. J. Vancso, and N. F. van Hulst, Phys. Rev. Lett. **91**, 038301 (2003).
[17] R. Vallee, M. Cotlet, J. Hotkens, and F. De Schryver, Macromolecules **36**, 7752 (2003).
[18] R. Vallee, M. Cotlet, M. Van Der Auweraer, J. Hofkens, K. Mullen, and F. De Schryver, J. Am. Chem. Soc. **126**, 2296 (2004).
[19] A. Schob, F. Cichos, J. Schuster, and C. von Borczyskowski, Eur. Polym. J. **40**, 1019 (2004).
[20] H. Uji-i, S. M. Melnikov, A. Deres, G. Bergamini, F. De Schryver, A. Hermann, K. Mullen, J. Enderlein, and J. Hofkens, Polymer **47**, 2511 (2006).
[21] D. G. Grier and C. A. Murray, J. Chem. Phys. **100**, 9088 (1994).
[22] A. H. Marcus and S. A. Rice, Phys. Rev. E **55**, 637 (1997).
[23] W. K. Kegel and A. van Blaaderen, Science **287**, 290 (2000).
[24] E. R. Weeks, J. C. Crocker, A. C. Levitt, A. Schofield, and D. A. Weitz, Science **287**, 627 (2000).
[25] E. R. Weeks and D. A. Weitz, Phys. Rev. Lett. **89**, 095704 (2002).
[26] R. E. Courtland and E. R. Weeks, J. Phys.: Condens. Matter **15**, S359 (2003).
[27] L. J. Kaufman and D. A. Weitz, J. Chem. Phys. **125**, 074716 (2006).
[28] W. Kob and H. C. Andersen, Phys. Rev. E **51**, 4626 (1995).
[29] W. Kob and H. C. Andersen, Phys. Rev. E **52**, 4134 (1995).
[30] W. Kob, C. Donati, S. J. Plimpton, P. H. Poole, and S. C. Glotzer, Phys. Rev. Lett. **79**, 2827 (1997).
[31] B. Doliwa and A. Heuer, Phys. Rev. Lett. **80**, 4915 (1998).
[32] C. Donati, J. F. Douglas, W. Kob, S. J. Plimpton, P. H. Poole, and S. C. Glotzer, Phys. Rev. Lett. **80**, 2338 (1998).
[33] B. Doliwa and A. Heuer, Phys. Rev. E **61**, 6898 (2000).
[34] G. Williams and P. J. Hains, Chem. Phys. Lett. **10**, 585 (1971).
[35] M. F. Shears and G. Williams, J. Chem. Soc., Faraday Trans. 2 **69**, 1050 (1973).
[36] F. R. Blackburn, M. T. Cicerone, G. Hietpas, P. A. Wagner, and M. D. Ediger, J. Non-Cryst. Solids **172**, 256 (1994).
[37] M. T. Cicerone, F. R. Blackburn, and M. D. Ediger, J. Chem. Phys. **102**, 471 (1995).
[38] M. T. Cicerone and M. D. Ediger, J. Chem. Phys. **104**, 7210 (1996).
[39] G. Heuberger and H. Sillescu, J. Phys. Chem. **100**, 15255 (1996).
[40] L. Wang and R. Richert, J. Chem. Phys. **120**, 11082 (2004).
[41] R. Bohmer, G. Hinze, G. Diezemann, B. Geil, and H. Sillescu, Europhys. Lett. **36**, 55 (1996).
[42] C. Y. Wang and M. D. Ediger, J. Phys. Chem. B **103**, 4177 (1999).
[43] A. J. Easteal, R. Mills, and L. A. Woolf, J. Phys. Chem. **93**, 4968 (1989).
[44] S. Bhattacharyya and B. Bagchi, J. Chem. Phys. **106**, 1757 (1997).
[45] S. Bhattacharyya and B. Bagchi, J. Chem. Phys. **107**, 5852 (1997).
[46] S. C. Glotzer, J. Non-Cryst. Solids **274**, 342 (2000).
[47] G. H. Koenderink, H. Y. Zhang, M. P. Lettinga, G. Nagele, and A. P. Philipse, Phys. Rev. E **64**, 022401 (2001).
[48] F. Ould-Kaddour and D. Levesque, Phys. Rev. E **63**, 011205 (2001).
[49] R. K. Murarka, S. Bhattacharyya, and B. Bagchi, J. Chem. Phys. **117**, 10730 (2002).
[50] E. Lindahl, B. Hess, and D. van der Spoel, J. Mol. Model. **7**, 306 (2001).
[51] H. J. C. Berendsen, J. P. M. Postma, W. F. Vangunsteren, A. Dinola, and J. R. Haak, J. Chem. Phys. **81**, 3684 (1984).
[52] E. Flenner and G. Szamel, Phys. Rev. E **72**, 011205 (2005).

[53] A. Widmer-Cooper and P. Harrowell, J. Phys.: Condens. Matter **17**, S4025 (2005).
[54] A. Widmer-Cooper and P. Harrowell, Phys. Rev. Lett. **96**, 185701 (2006).
[55] K. Kerl and M. Willeke, Mol. Phys. **97**, 1255 (1999).
[56] M. Willeke, Mol. Phys. **101**, 1123 (2003).
[57] J. R. Schmidt and J. L. Skinner, J. Chem. Phys. **119**, 8062 (2003).
[58] J. R. Schmidt and J. L. Skinner, J. Phys. Chem. B **108**, 6767 (2004).
[59] P. Scheidler, W. Kob, and K. Binder, Europhys. Lett. **59**, 701 (2002).
[60] P. Scheidler, W. Kob, and K. Binder, Eur. Phys. J. E **12**, 5 (2003).
[61] P. Scheidler, W. Kob, and K. Binder, J. Phys. Chem. B **108**, 6673 (2004).
[62] J. Baschnagel and F. Varnik, J. Phys.: Condens. Matter **17**, R851 (2005).
[63] F. Varnik, J. Baschnagel, and K. Binder, Phys. Rev. E **65**, 021507 (2002).
[64] T. Fehr and H. Lowen, Phys. Rev. E **52**, 4016 (1995).